Supporting Information

Synthetic styrene-based bioinspired model of the [FeFe]-hydrogenase active site for electrocatalytic hydrogen evolution

Afridi Zamader,[1,2,+] Bertrand Reuillard,[1] Julien Pérard,[1] Laurent Billon,[3,4] Gustav Berggren[2] and Vincent Artero[1]

[1] Univ. Grenoble Alpes, CNRS, CEA, IRIG, Laboratoire de Chimie et Biologie des Métaux, 17 rue des Martyrs, 38000 Grenoble, France.

[2] Department of Chemistry- Ångström Laboratory, Uppsala University, Box 523, SE-75120 Uppsala, Sweden.

[3] Universite de Pau et des Pays de l'Adour, E2S UPPA, CNRS, IPREM, 64053 Pau, France.

[4] Universite de Pau et Pays de l'Adour, E2S UPPA, Bio-inspired Materials Group: Functionalities & Self-Assembly, 64053 Pau, France.

+ current address: Université Paris Cité, Laboratoire d'Electrochimie Moléculaire, CNRS, F-75006, Paris, France.

Table of Contents

1. Materials

All chemicals were purchased from Sigma-Aldrich. Multiwall carbon nanotubes (MWNT) were purchased from NANOCYL® NC7000™ series. The organic solvents used for synthesis, spectroscopy and electrochemical assessment were anhydrous and degassed. The glassware used were dried overnight in oven (120^0C) before each reaction. All Synthesis were performed under Schlenk line under Argon or N_2.

2. Methods

NMR (^{1}H and ^{13}C) spectroscopy was performed in Bruker AVANCE III–500 MHz and JEOL solution–400 MHz spectrometer by dissolving the compounds in deuterated solvents contain 0.05% Tetramethyl silane (TMS) as internal standard. Mass spectrometry were performed using Thermo Scientific LXQ mass spectrometer equipped with an electrospray source, at Service de Chimie Inorganique et Bioinorganique of CEA-Grenoble/CNRS (Grenoble, France). High-resolution/accurate mass measurements (HRAM*)* were performed on a Q-TOF mass spectrometer by the SALSA platform from ICOA laboratory.

2.1 UV-vis measurements

UV–vis spectroscopy was accomplished using a Shimadzu UV-1800 spectrophotometer with dual beam mode. The samples were dissolved in anhydrous solvent (dimethylformamide or DMF in our study) and analyzed in quartz made cuvette with 1 cm of path length.

2.2 FTIR measurements

The Infrared spectroscopy was conducted using two different modes: transmission and attenuated total reflection (ATR). The transmission mode measurements were performed using a PerkinElmer Spectrum spectrometer, while the ATR mode measurements were carried out using a Bruker Vertex V70v spectrometer. For the transmission mode, a transmission cell made of CaF_2 with a spacer of 0.05 nm thickness was utilized. The ATR mode measurements employed an ATR cell (specifically, the BioRad II model from Harrick scientific) sealed with

a custom-built PEEK cell. In the ATR mode, the sample was dissolved in different buffers with a concentration of 100 mg mL^{-1}, and a 2 µL of the resultant mixture was drop casted onto the ATR crystal for the measurements.

2.3 Size exclusion chromatography

Size exclusion chromatography (SEC) was performed at Université de Pau et des Pays de l'Adour (UPPA) using machine equipped with 4 columns performed (Shodex KF 801, 802.5, 804 and 806) of size (I.D.×Length) of 8 µm × 300 mm and a precolumn (Shodex KFG) of 4.6 × 8 mm with a detector of viscosimeter Malvern VE3580 at 30°C. DMF was used as eluent with 1 mL min^{-1} flowrate with polystyrene as a standard for reference.

2.4 Electrochemical measurements

The electrochemical assessments were accomplished with a Biologic SP-300 workstation at room temperature (298K) under argon atmosphere. The working electrode (*i.e.*, glassy carbon) was polished using Struers LaboPol-1 polishing machine with diamond paste (d= 1 µM) followed by rinsing with water and ethanol and dried before experiments. A platinum coil and Ag/AgCl (3M KCl) were used as counter and reference electrode, respectively. The multi-walled carbon nanotubes (MWNT) suspension was prepared using Bandelin Sonorex sonication bath. The CV traces were plotted by calculating potential value against Ferrocene/Ferrocenium ($Fc^{+1/0}$) and reversible hydrogen electrode (RHE) redox potential as standard for organic media and for aqueous media, respectively. The CV under aqueous condition (both homogenous and heterogeneous) was measured using the ohmic drop compensation method (ZIR) from EC-Lab, compensating for 85% of the measured R_u.

2.5 Product detection

Gas chromatography was conducted using Micro Gas Chromatograph S3000 (SRA Instruments) with a diamond LV Ms5A 14m module, operated using the Soprane chrome interface. Argon was used as feeding gas with flowrate of 5 mL min^{-1}, controlled via Bronkhorst EL-FLOW mass-flow meter.

2.6 Metal content analysis

Sample were mineralized in 65% nitric acid overnight prior to analysis by inductively coupled plasma atomic emission spectroscopy (ICP-AES) on a Shimadzu ICP 9000 with Mini plasma Torch instrument used in axial reading mode. A standard range of iron (from 3.9 µg/L to 1 mg/L) was prepared extemporaneously for quantification with a correlation coefficient of 0.999. Specific wavelength of 259.940 nm was chosen to be more accurate and minimize spectral interference ray. All measurements were done in triplicate with a RSD under 0.5.

2.7 Sample preparation

The sample for metallopolymers functionalized MWNT based working electrode, bulk electrolysis, and post operando UV-vis were prepared using a previously reported protocol.[1] Briefly, 20µL of a 3 mg mL^{-1} of MWNT suspension in ethanol were drop casted at the surface of a glassy carbon electrode (d = 1.6 mm) and allowed to dry for 30 min. The MWNT modified electrode was then soaked in solution of the metallopolymers (**1a**, **1b**, **1c**) and complex **2** in DMF at concentration of 15 mg mL^{-1} (0.9-1 mM) and 2.7 mg mL^{-1} (~3.6 mM), respectively, for 15 min. Subsequently, the catalysts modified electrodes were washed with DMF and milliQ water prior to their use under electrochemical/catalytic conditions.

2.8 Rinse test

The rinse test was performed using three CV scan. The first scan was performed by using a fresh glassy carbon electrode (GCE, d=1.6 mm) in 0.2 M sodium phosphate buffer, pH 7 under argon called "blank". Subsequently, another CV scan was performed with a fresh GCE but in mixture of metallopolymers dissolved in aforementioned buffer called "scan 1". The GCE after the scan 1 was then collected and gently rinsed with water followed by running another CV scan in a buffered deprived of metallopolymers to obtain "scan 2" (see Figure S18).

2.9 Synthesis

1a: Complex **1** or $[Fe_2(\mu–SCH_2N(CH_2C_6H_4CHCH_2)CH_2S–)(CO)_6]$[2] and 4-(pyren-1-yl)-butyl methacrylate (PyBMA)[1] were synthesized as per previously reported protocols. Subsequently, 36 mg (0.071 mM) of complex **1**, 24.3 mg (0.071 mM) of PyBMA and 6.5 mg (0.039 mM) Azobisisobutyronitrile (AIBN) were placed in a dry, degassed Schlenk flask and flush with N_2 atmosphere and dissolved in 2.4 mL of anhydrous, degassed toluene. Then, 1.2 mL (7.1 mM)

DMAMEA was then added dropwise and the solution was degassed from O_2 by 3 freeze-pump-thaw cycles. The schlenk flask was then dipped in a pre-heated oil bath at 70 °C and stirred overnight (12 hours) at 70 °C. After cooling to room temperature, the resulted viscous mixture was precipitated by dropping dark brown solution into 50 mL of hexane. The sticky solid was washed with 20 mL of hexane to remove unreacted reagents and low molecular weight compounds, affording a white solid product, which was then dried under high vacuum to yield 0.7 g of brown/orange colored solid. yield was ~60%. ^{1}H NMR (CD_2Cl_2, 500 MHz, 298 K) δ (ppm): 8.4–7.9 (broad, aromatic group from pyrene), 7.3–7.0 (4H, aromatic group of styrene, broad), 4.03 (2H, –O**CH_2**$CH_2N(CH_3)_2$, t), 3.42 (2H, –O**CH_2**$CH_2CH_2CH_2$–$C_{16}H_9$), 2.54 (2H, –OCH_2**CH_2**$N(CH_3)_2$, t), 2.25 (6H,–OCH_2CH_2N(**CH_3**$)_2$, s), 2.20 (4H, –OCH_2**CH_2CH_2**CH_2–$C_{16}H_9$) 2.0–1.8 (2H, aliphatic main chain and 3H from terminal methyl group of linker, broad), 1.5–1.26 (methyl, end group, broad) 1.1–0.7 (3H, –CH_3, main chain, broad) (Figure S2). IR ($CHCl_3$, thin film on CaF_2) wavenumber (cm^{-1}): 2950 (C–H stretching, sharp), 2827 (C-–H stretching of –$N(CH_3)_2$, sharp), 2779 (C–H stretching of –$N(CH_3)_2$, sharp), 2074 (Fe–CO, sharp), 2036 (Fe–CO, sharp), 2001 (Fe–CO, sharp), 1726 (–C=O of ester bonds) and 1153 (C–N stretching, strong) (Figure 1C, S12). UV–vis (DMF), λ (nm): 217–350 (π–π*, sharp, multiple peaks due to aromatic ring of pyrene) (Figure 1B). DMF GPC: $M_{n,\ SEC}$ = 14,200 g/mol, M_w/M_n = 2.7 (Figure S16A).

1b: Synthesis of **1b** was accomplished by following same procedures as mentioned for **1a** except varying stoichiometric composition as mentioned in Table S1. Yield was 0.76 g (~60%).^{1}H NMR (CD_2Cl_2, 500 MHz, 298 K) δ (ppm): 8.4–7.9 (aromatic group from pyrene, broad), 7.3–7.1 (4H, aromatic group of styrene, broad), 4.04 (2H, –O**CH_2**$CH_2N(CH_3)_2$,t) 3.42 (2H, –O**CH_2**$CH_2CH_2CH_2$–$C_{16}H_9$), 2.55 (2H,–OCH_2**CH_2**$N(CH_3)_2$, t), 2.25 (6H,–OCH_2CH_2N(**CH_3**$)_2$, s), 2.20 (4H, –OCH_2**CH_2CH_2**CH_2–$C_{16}H_9$), 2.0–1.8 (2H, broad, aliphatic main chain and 3H from terminal methyl group of linker), 1.46–1.26 (broad, methyl, end group) 1.1–0.7 (3H, broad, –CH_3, main chain) (Figure S3). IR ($CHCl_3$, thin film on CaF_2) wavenumber(cm^{-1}): 2950 (C–H stretching, sharp), 2827 (C–H stretching of –$N(CH_3)_2$, sharp), 2779 (C–H stretching of –$N(CH_3)_2$, sharp), 2074 (Fe–CO, sharp), 2036 (Fe–CO, sharp), 2001 (Fe–CO, sharp), 1726 (–C=O of ester bonds) and 1153 (C–N stretching, strong) (Figure 1C, S12). UV–vis (DMF), λ(nm): 217–350 (π–π*, sharp, multiple peaks due to aromatic ring of pyrene) (Figure 1B). DMF GPC: $M_{n,\ SEC}$ = 16,650 g/mol, M_w/M_n = 2.19 (Figure S16B).

1c: Synthesis of **1c** was executed by following same procedures as mentioned for **1a** except varying stoichiometric composition as mentioned in Table S1. Yield was 1.1 g (~78%).^{1}H

NMR (CD_2Cl_2, 500 MHz, 298 K) δ (ppm): 8.31–7.94 (broad, aromatic group from pyrene), 7.3–7.12 (broad, aromatic group of styrene), 4.06 (2H,–O**CH$_2$**$CH_2N(CH_3)_2$, t), 3.42 (2H, –O**CH$_2$**$CH_2CH_2CH_2$–$C_{16}H_9$), 2.57 (2H, –OCH_2**CH$_2$**$N(CH_3)_2$, t), 2.25 (6H, –OCH_2CH_2N(**CH$_3$**)$_2$, s), 2.2 (4H, –O**CH$_2$CH$_2$**CH_2CH_2–$C_{16}H_9$) 2.1–1.6 (2H, aliphatic main chain and 3H from terminal methyl group of linker, broad), 1.52–1.25 (broad, methyl, end group) 1.1–0.7 (3H, broad, –CH_3, main chain) (Figure S4). IR ($CHCl_3$, thin film on CaF_2) wavenumber(cm^{-1}): 2950 (C–H stretching, sharp), 2827 (C–H stretching of –$N(CH_3)_2$, sharp), 2779 (C–H stretching of –$N(CH_3)_2$, sharp), 2074 (Fe–CO, sharp), 2036 (Fe–CO, sharp), 2001 (Fe–CO, sharp), 1726 (–C=O of ester bonds) and 1153 (C–N stretching, strong) (Figure 1C, S12). UV–vis (DMF) λ(nm): 217–350 (π–π*, sharp, multiple peaks due to aromatic ring of pyrene) (Figure 1B). DMF GPC: $M_{n,\,SEC}$ = 17,300 g/mol, M_w/M_n = 2.25 (Figure S16C).

Table S1: **Stoichiometric recipe used for synthesis of 1a–c.**

Metallopolymers	Chemical name	mM	Equivalents	Mass/Volume	Mass of the product obtained
1a	Complex **1**	0.071	1	36 mg	0.7 g
	DMAEMA	7.1	100	1.2 mL	
	Pyrene linker	0.071	1	24.3 mg	
	AIBN	0.039	0.55	6.5 mg	
	Toluene			2.4 mL	
1b	Complex **1**	0.071	1	36 mg	0.76 g
	DMAEMA	7.1	100	1.2 mL	
	Pyrene linker	0.355	5	121.5 mg	
	AIBN	0.039	0.55	6.4 mg	
	Toluene			2.5 mL	
1c	Complex **1**	0.071	1	36 mg	1.1 g
	DMAEMA	7.1	100	1.2 mL	
	Pyrene linker	0.71	10	243 mg	
	AIBN	0.039	0.55	6.5 mg	
	Toluene			2.7 mL	

1' : The synthesis of complex **1'** was achieved by employing a slightly modified methodology based on a previous report[3]. Initially, a solution of $Fe_2(\mu\text{-}S_2)(CO)_6$ (0.34 g, 1.00 mmol) in 20 mL of anhydrous , degassed THF was prepared under argon, resulting in a red-colored solution. This solution was then cooled to -78 °C, followed by the addition of 2.0 mL of super-hydride

solution (Et_3BHLi), resulting in a dark green-colored solution. The mixture was stirred for 15 minutes at –78 °C before introducing 0.2 mL (2.0 mmol) of CF_3COOH. After stirring for 15 minutes at room temperature (25 °C), the solution turned dark red. Subsequently, 0.16 mL (2.0 mmol) of aqueous CH_2O (37%) was added and stirred for 1.5 hours at room temperature. Then, 0.15 g (1.0 mmol) of 4-(Aminomethyl) benzoic acid was added, and the resulting suspension was stirred for 4.5 hours at 37 °C. The mixture was then evaporated under reduced pressure and extracted with $CHCl_3$. The extracted solution, which exhibited a red color, was filtered and concentrated to obtain approximately 0.45 g of dark red solid. This solid was characterized by FTIR and ^{1}H NMR spectroscopy without further purification. The yield of the synthesis was approximately 90% (Scheme S2). ^{1}H NMR (CD_3CN, 400 MHz, 298 K) δ (ppm): 7.94 (2H, aromatic proton of styrene, d, j = 8.0 Hz), 7.31 (2H, aromatic proton of styrene, d , j = 8.0 Hz), 3.86 (2H, –C_6H_4**CH_2**N–, s), 3.47 (4H,–N**CH_2CH_2**S_2–, s) (Figure S6). IR ($CHCl_3$, thin film on CaF_2) wavenumber (cm^{-1}): 2075 (Fe–CO, sharp), 2037 (Fe–CO, sharp), 2002 (Fe–CO, sharp), 1707 (–C=O of carboxylic acid) (Figure S15, blue trace).

2: 0.21 g (0.4 mmol) of complex **1'**, along with 0.17 g (0.64 mmol) of 1-Pyrenemethylamine hydrochloride, 92 mg (0.8 mmol) of N-hydroxysuccinimide, and 123 mg (0.64 mmol) were dissolved in 20 mL of degassed, anhydrous dichloromethane. Subsequently, 110 µL (0.64 mmol) of N-diisopropylethylamine was added to the resulting mixture, which was then stirred for 14 hours at room temperature (25 °C). The mixture was extracted with 100 mL of dichloromethane and washed with 100 mL of a brine solution. The organic layer was collected, dried with anhydrous sodium sulfate, and concentrated under reduced pressure to obtain a red-colored solid. The obtained solid was further purified using column chromatography with an ethyl acetate-hexane solvent system. The elute was concentrated, resulting in 120 mg of brick-red solid. The overall yield of the purification process was approximately 50% (Scheme S2). ^{1}H NMR (DMSO-d6, 400 MHz, 298 K) δ (ppm): 9.2 (1H, –CH_2**NH**–, t, j = 4.0 Hz) 8.5–8.0 (multiple peaks from pyrene), 7.88 (2H, aromatic proton of styrene, d, j = 8.0 Hz), 7.29 (2H, aromatic proton of styrene, d, j = 8.0 Hz), 5.22 (2H, –**CH_2**NHCOC_6H_4–, d , j = 8.0 Hz), 3.88 (2H, –C_6H_4**CH_2**N– , s), 3.56 (4H,–N**CH_2CH_2**S_2–, s)(Figure S7). ^{13}C NMR (DMSO-d6, 400 MHz, 298 K) δ (ppm): 208.6 (**C**O–Fe), 170.9 (–NH**C**O–), 166.4 – 123.8 (from aromatic group at bridgehead styrene and pyrene), 60.2 (–$C_{16}H_9$**CH_2**NH–), 52.6 (–C_6H_4**CH_2**N–), 26.1 (–N**CH_2CH_2**S_2–) (Figure S8). IR ($CHCl_3$, thin film on CaF_2) wavenumber (cm^{-1}): 2075 (Fe–CO, sharp), 2037 (Fe–CO, sharp), 2002 (Fe–CO, sharp), 1659 (–C=O of amide linkage) (Figure S15, orange trace). UV–vis (DMF) λ(nm): 217–350 (π–π*, sharp, multiple peaks due to

aromatic ring of pyrene), 450-500 (σ-σ*, broad, Fe–S bonds) (Figure 1B). High-resolution mass spectra (HRMS): Calculated for $C_{33}H_{22}Fe_2N_2O_7S_2$: 733.96; found : 734.96 $[M+H]^+$ (Figure S9).

2.10 Calculation

The normalization of each cyclic volumetric experiment against reference electrode, active site loading , turnover number (TON_{H2}) and turnover frequency (TOF_{H2}) for hydrogen production, Faradic efficiency (FE) during CA were estimated following previously reported methods.[1] The surface loading via CV assessments were estimated using quasi-reversible signal at ~$E_{1/2} \approx -1.55$ to -1.63 V *vs.* $Fc^{+1/0}$ as 1 e^- reduction event (*i.e.* Fe^IFe^I/Fe^IFe^0) (Figure S21-24).

The surface loading of the active site via ICP-OES (in mol cm^{-2}) =

$$\frac{X_{Fe}}{A \times 2 \times mol\ wt.\ of\ Fe}$$

Here, X_{Fe} = the amount of Fe present of electrode surface (in g). A =surface area of the subjected electrode used for ICP-OES measurements (in cm^2); mol wt. of Fe = 55.85 g/mol.

3.Figures and Tables

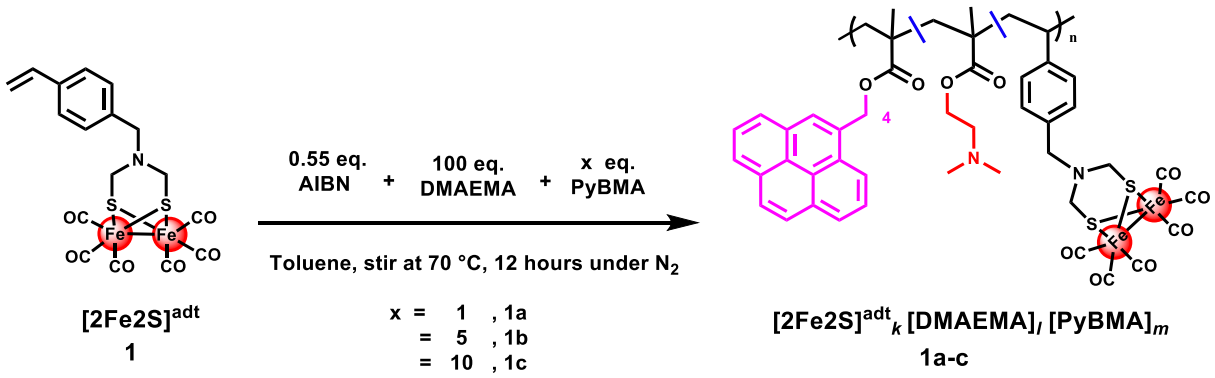

Scheme S1: Synthesis scheme of metallopolymers **1a –c**. Here, k: l: m represents the ratio $[2Fe2S]^{adt}$:[DMAEMA]:[PyBMA]. The exact details of the ratio for each metallopolymers were mentioned in **Table 1**.

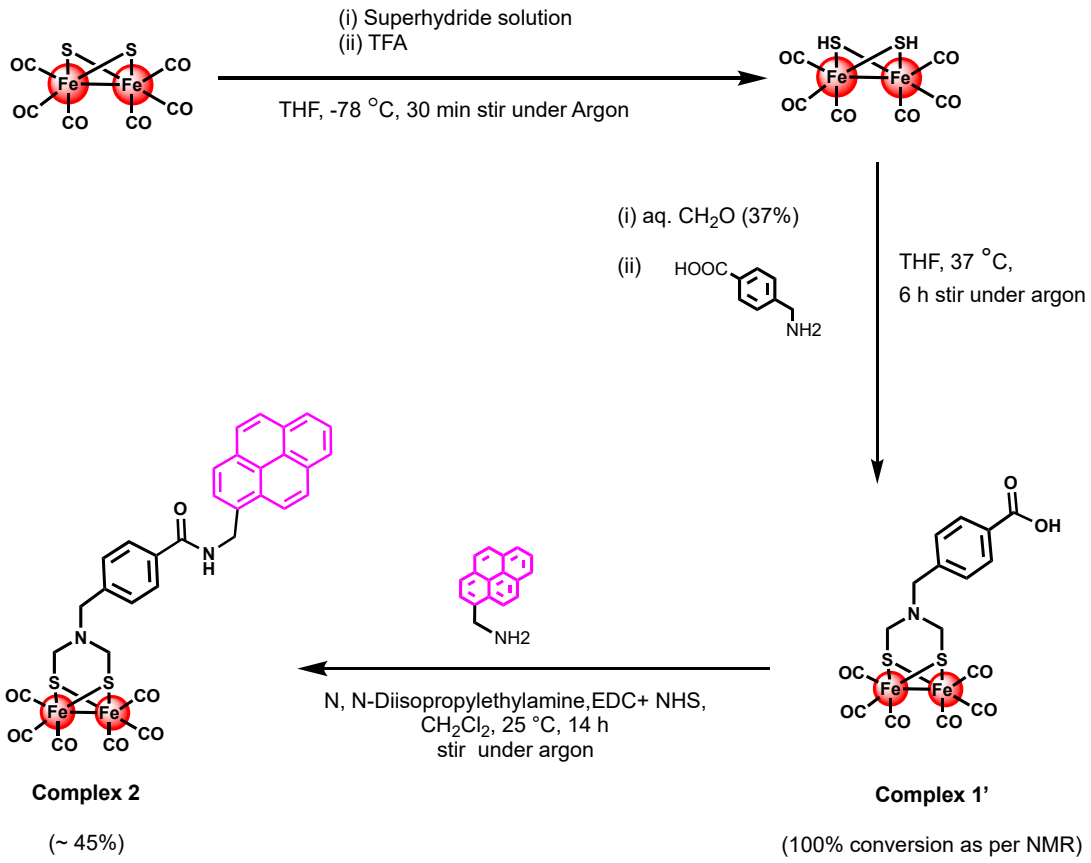

Scheme S2: Synthesis scheme of complex **2**. Here, TFA = trifluoracetic acid, EDC = 1-Ethyl-3-(3-dimethylaminopropyl)carbodiimide and NHS = N-Hydroxysuccinimide.

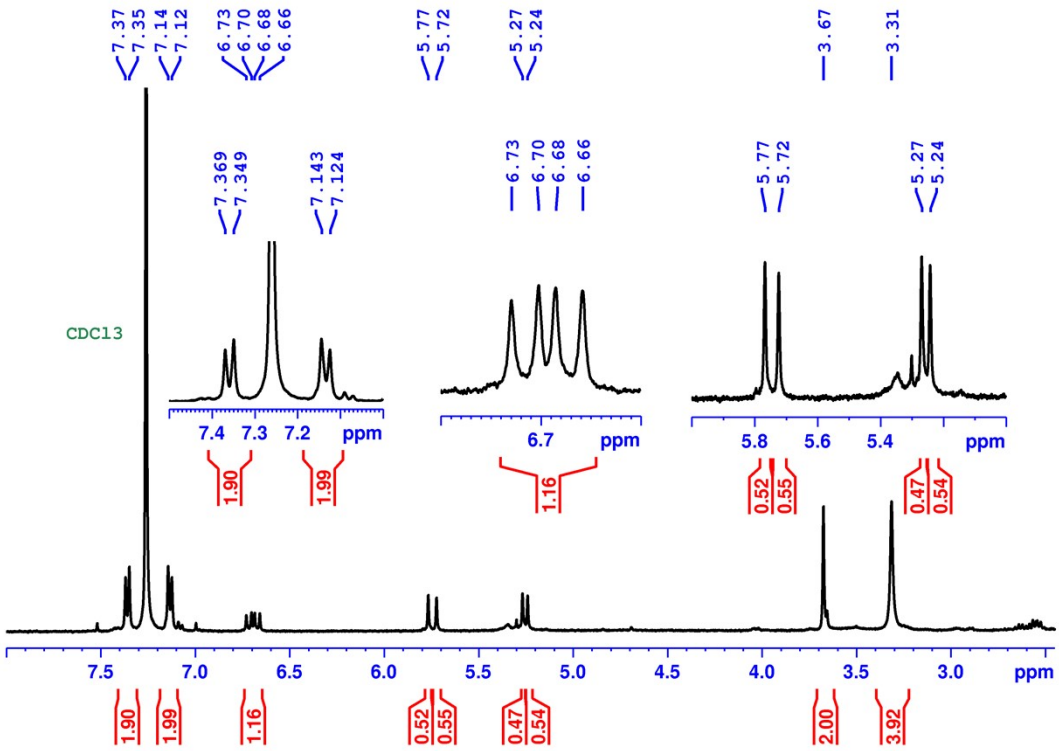

Figure S1: ^{1}H NMR of complex **1** in $CDCl_3$.

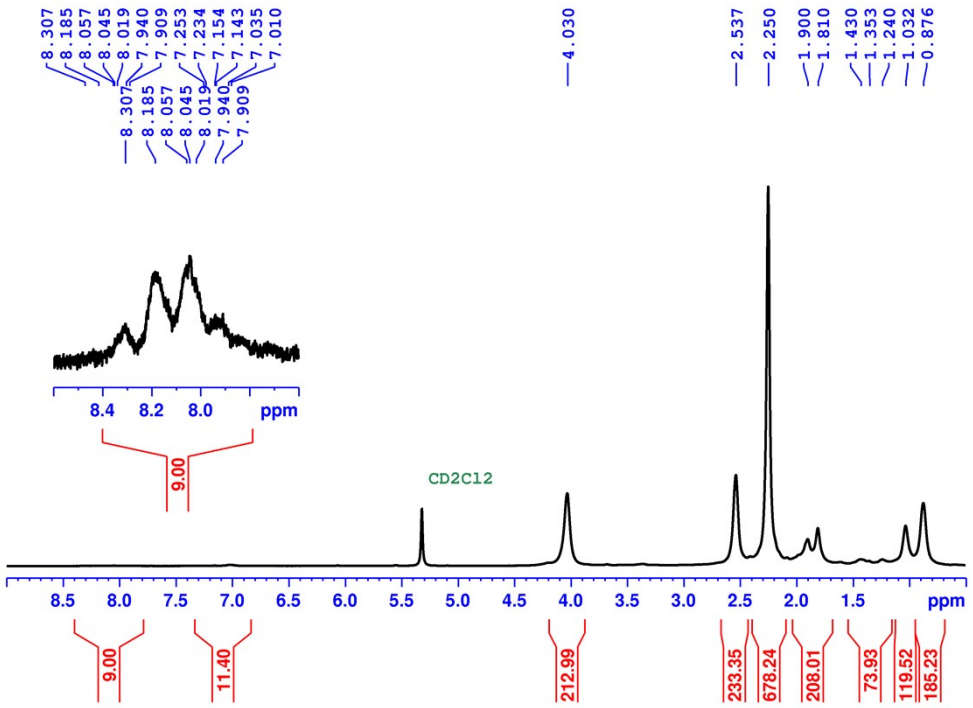

Figure S2: ^{1}H NMR of metallopolymer **1a** in CD_2Cl_2.

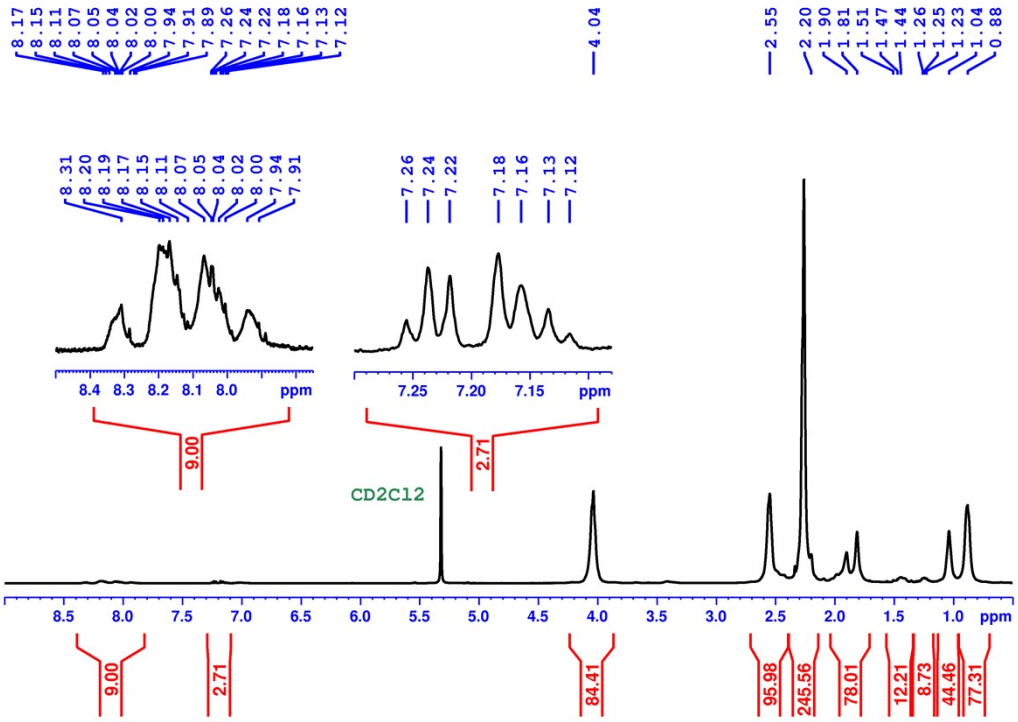

Figure S3: ^{1}H NMR of metallopolymer **1b** in CD_2Cl_2.

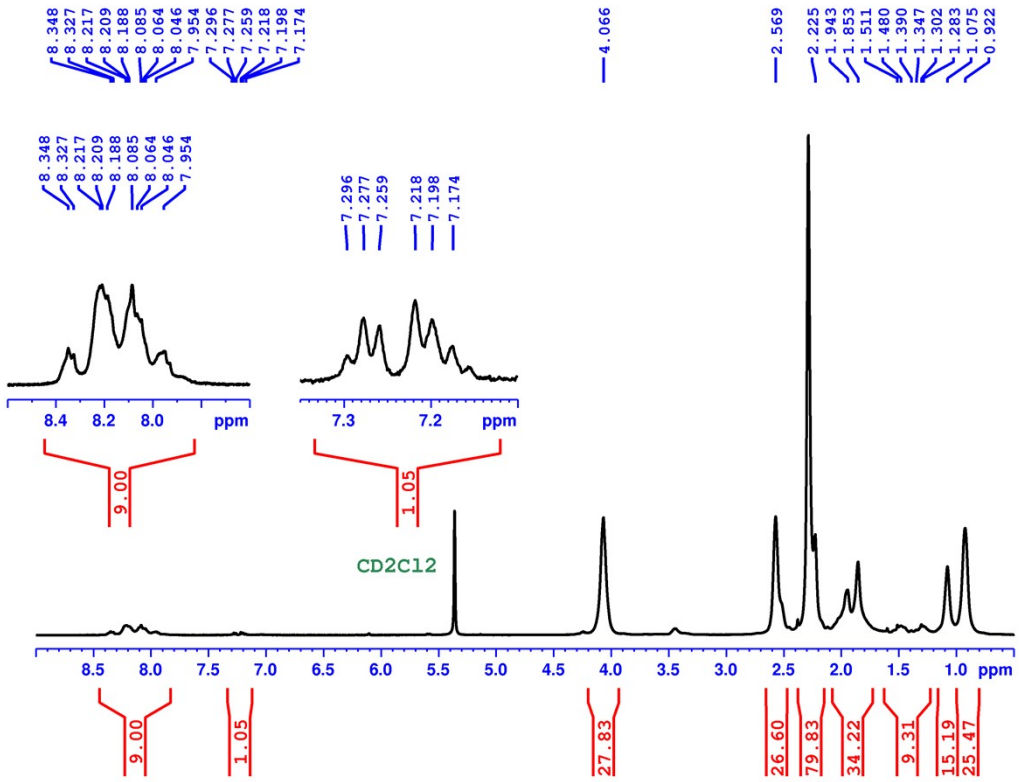

Figure S4: ^{1}H NMR of metallopolymer **1c** in CD_2Cl_2.

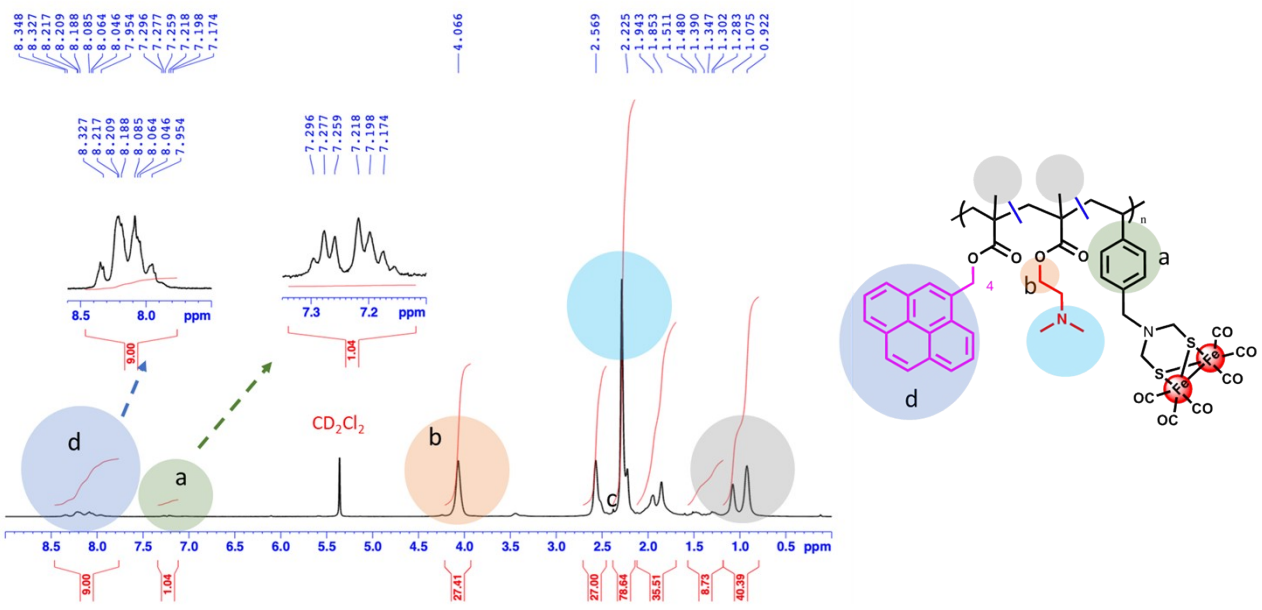

Figure S5: Analysis of ^{1}H NMR peak based on different monomers presents in metallopolymers **1a –c**.

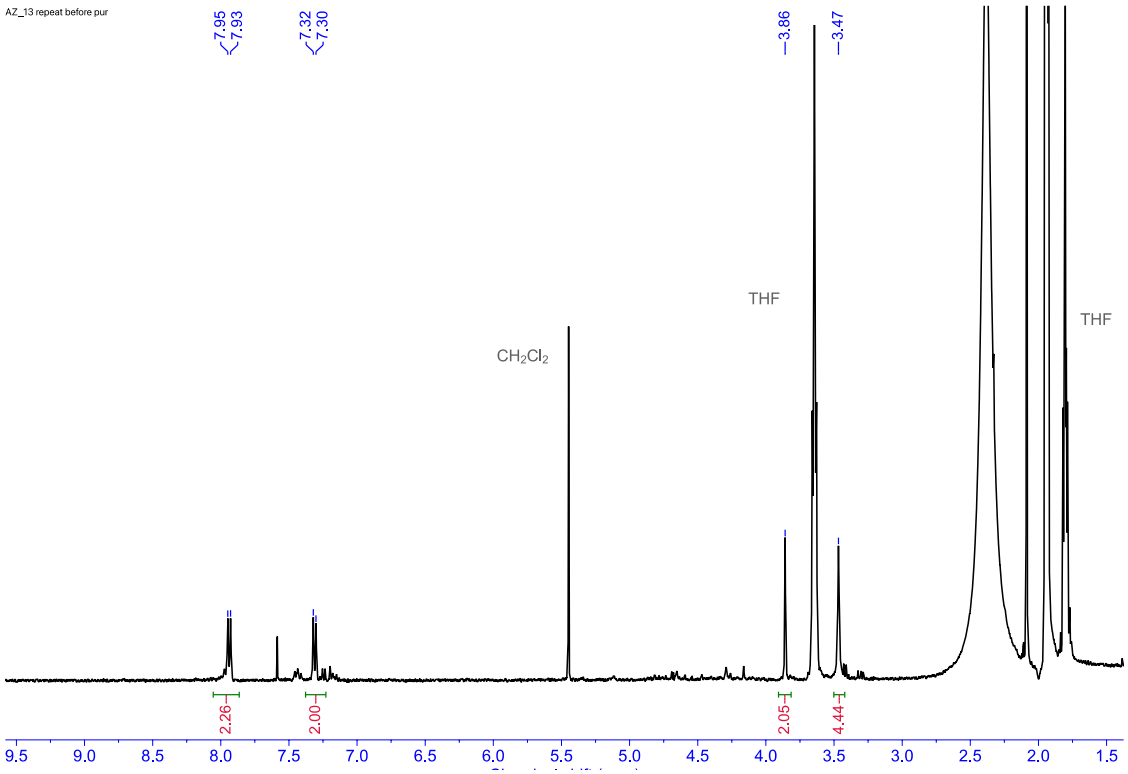

Figure S6: ^{1}H NMR of complex **1'** in CD_3CN.

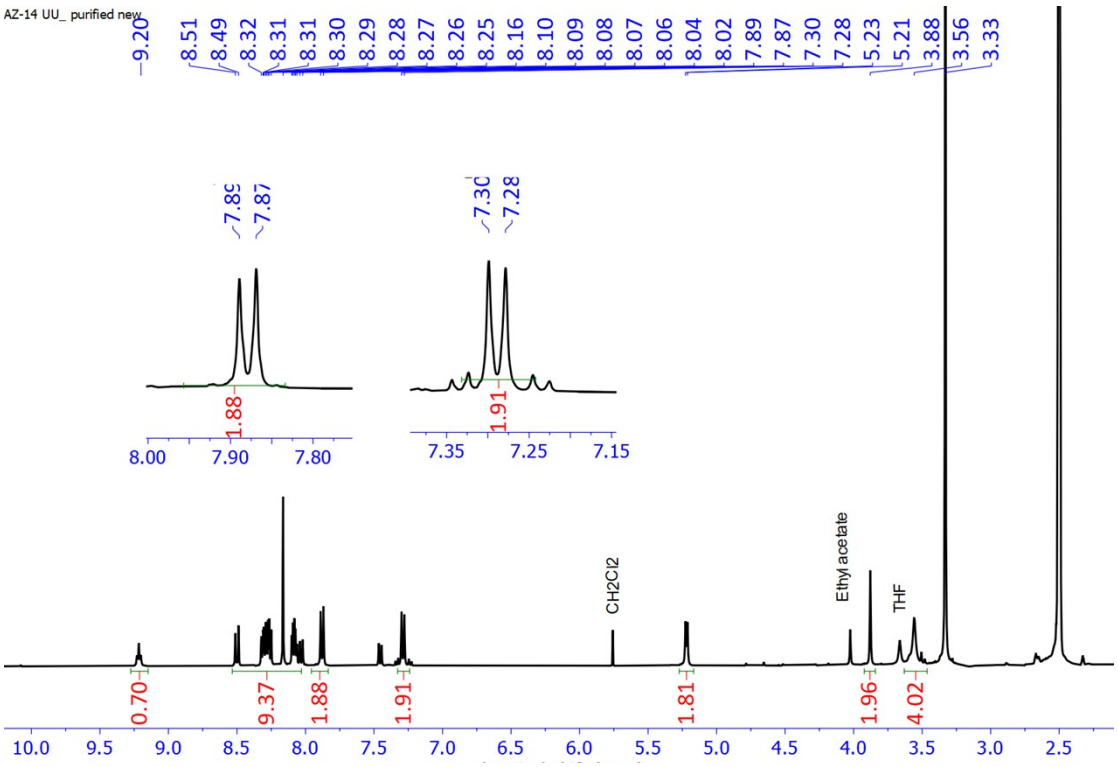

Figure S7: ^{1}H NMR of complex **2** in DMSO-d_6.

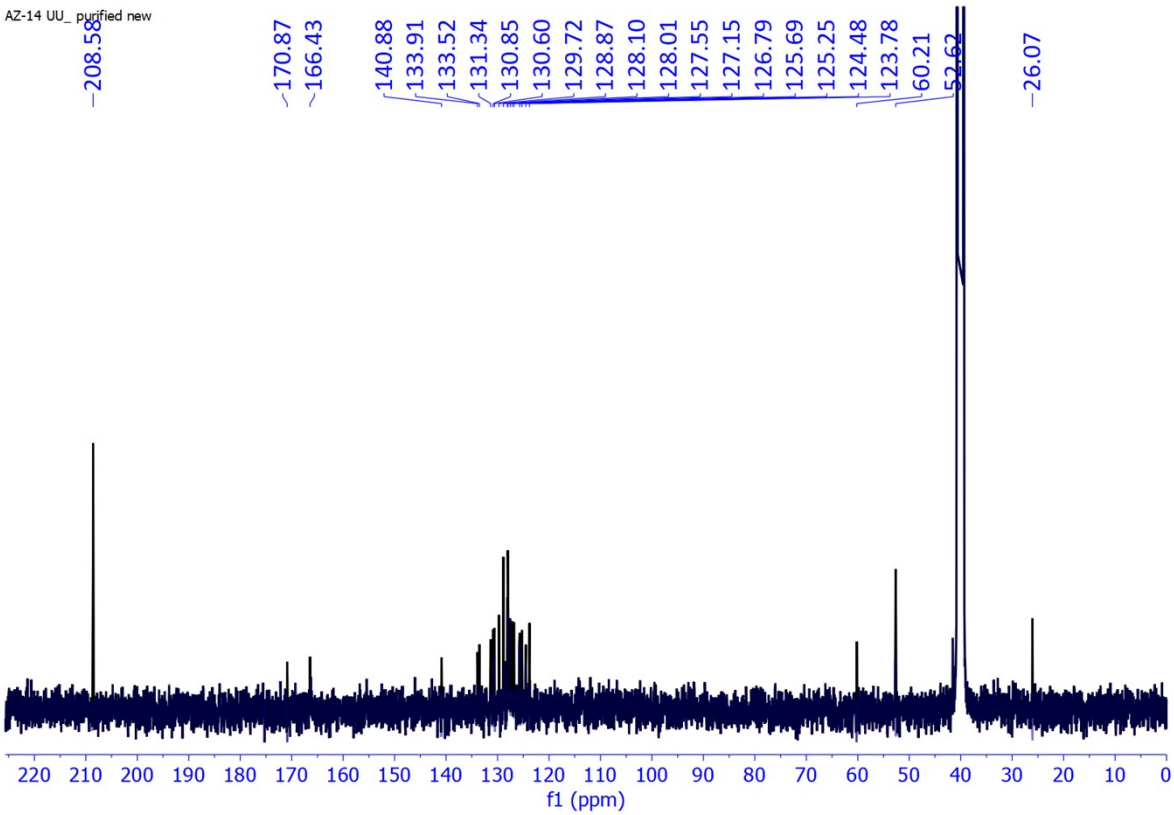

Figure S8: ^{13}C NMR of complex **2** in DMSO-d_6.

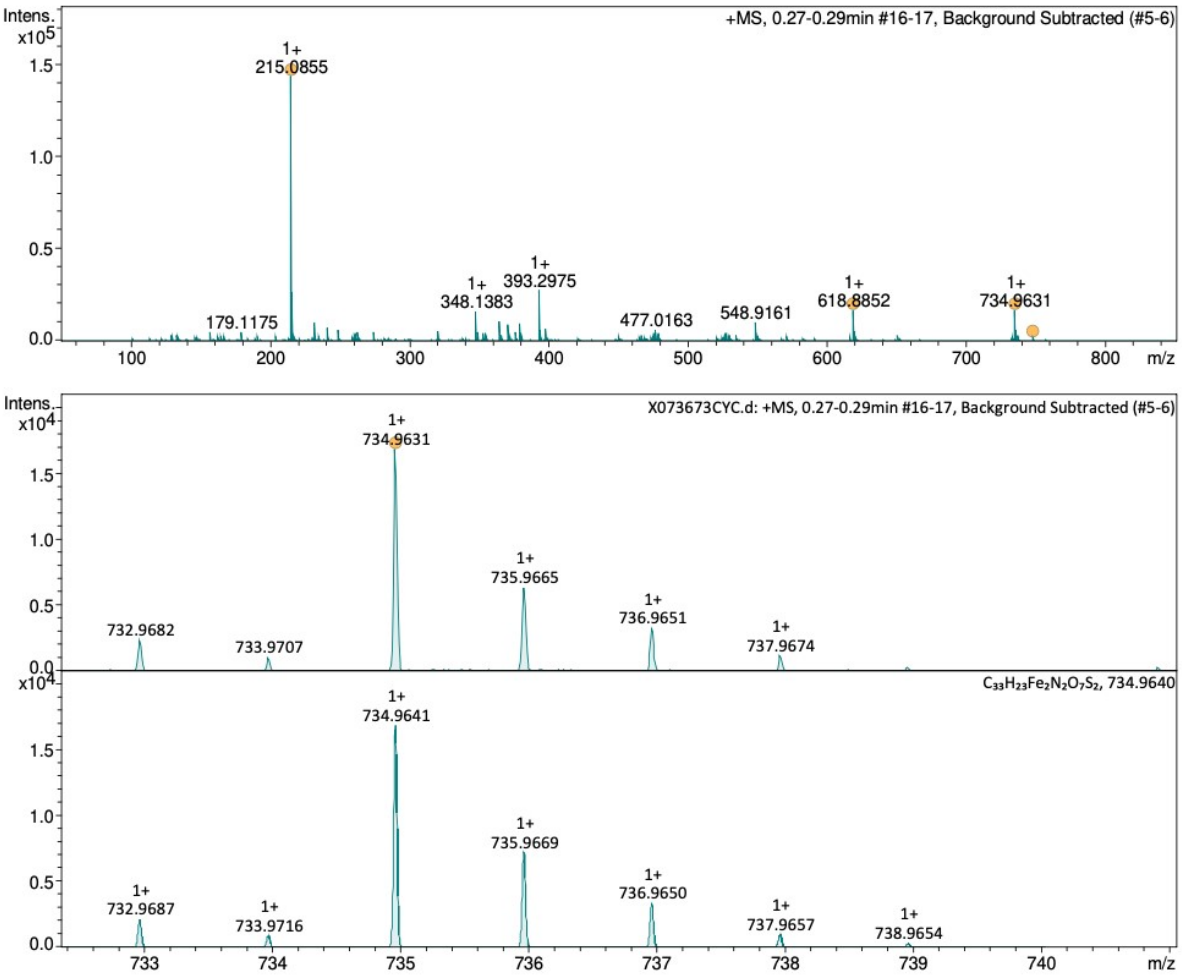

Figure S9: High resolution mass spectrometry (HRMS) of complex **2.** Calculated for $C_{33}H_{22}Fe_2N_2O_7S_2$: 733.96 ; found : 734.96 $[M+H]^+$.

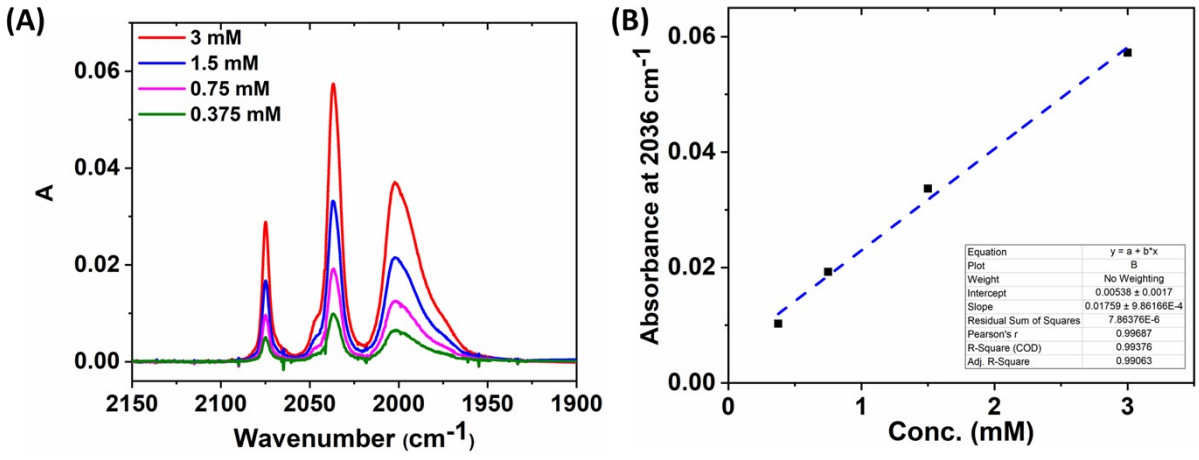

Figure S10: Infrared spectra (transmission mode) of Complex **1** at different concentration in $CHCl_3$. (A) at concentration range between 0.375–3 mM and (B) and linear plot of background subtracted absorption of peak at 2036 cm^{-1} *vs.* concentration. The analysis was performed in transmission cell with path length of 0.05 nm. The extinction coefficient (ε) was calculated 352 ± 20 $M^{-1}mm^{-1}$ for 2036 cm^{-1}.

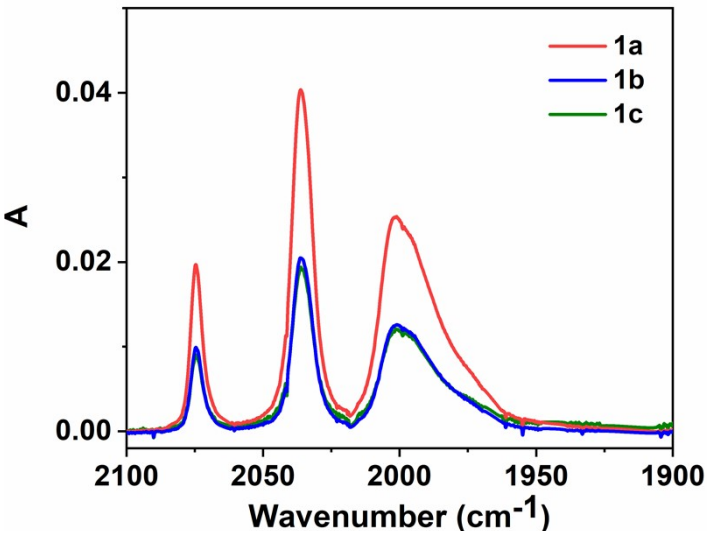

Figure S11: Infrared spectra (transmission mode) of metallopolymers **1a–c** at different concentration in $CHCl_3$ with 20 mg per ml concentration. The analysis was performed in transmission cell with path length of 0.05 nm.

Table S2: **Details of mol of active sites present per mol of metallopolymers from ICP -OES and Infrared spectra measure from Figure S10 and S11.**

Metallopolymers	**Fe content[a]** **(mg_{Fe}/g of polymer)**	**Moles of active sites per mol of metallopolymers As per ICP-OES measurement** **(mol)**	**Moles of active sites per mol of metallopolymers as Infrared spectra measurement** **(mol)**
1a	9.6 ± 0.2	1.21	1.53 ± 0.1
1b	4.10 ± 0.06	0.6	0.96 ± 0.05
1c	4.0 ± 0.1	0.62	0.95± 0.05

a : measured by ICP-OES

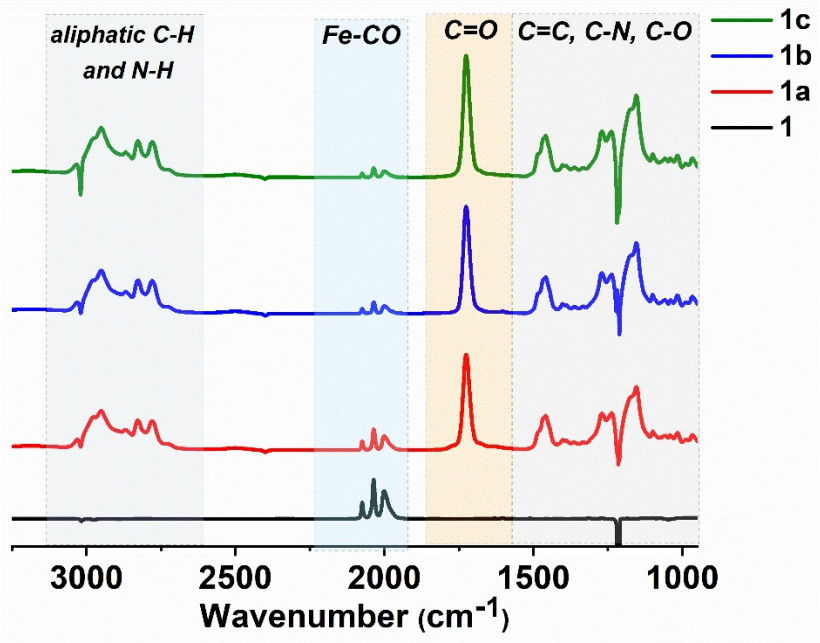

Figure S12: Infrared spectroscopy (transmission mode) of **1** and **1a–c** in $CHCl_3$ using transmission mode. Plots for **1**, **1a**, **1b** and **1c** are represented with black, red, blue and green colors respectively. The intensity of traces of metallopolymers **1a–c** are multiplied between 2–5 times as compared to complex **1** for better comparison.

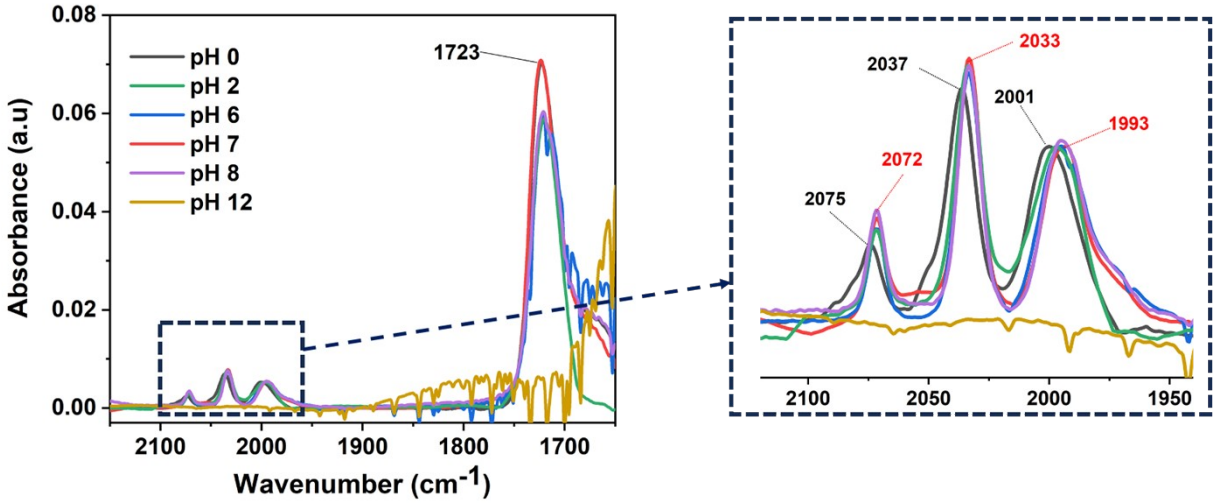

Figure S13: Infrared spectra (ATR mode) of metallopolymer **1b** at different pH with concentration of 100 mg mL^{-1}. pH 0 (black trace), pH 2 (green trace), pH 6 (blue trace), pH 7 (red trace), pH 8 (purple trace) and pH 12 (yellow trace).The metallopolymer was insoluble at pH 12. For the preparation of the buffers from pH 2, 6, 7, 8 and 12, 0.2 M sodium phosphate buffer was used. For pH 0, 0.5 M H_2SO4 was used.

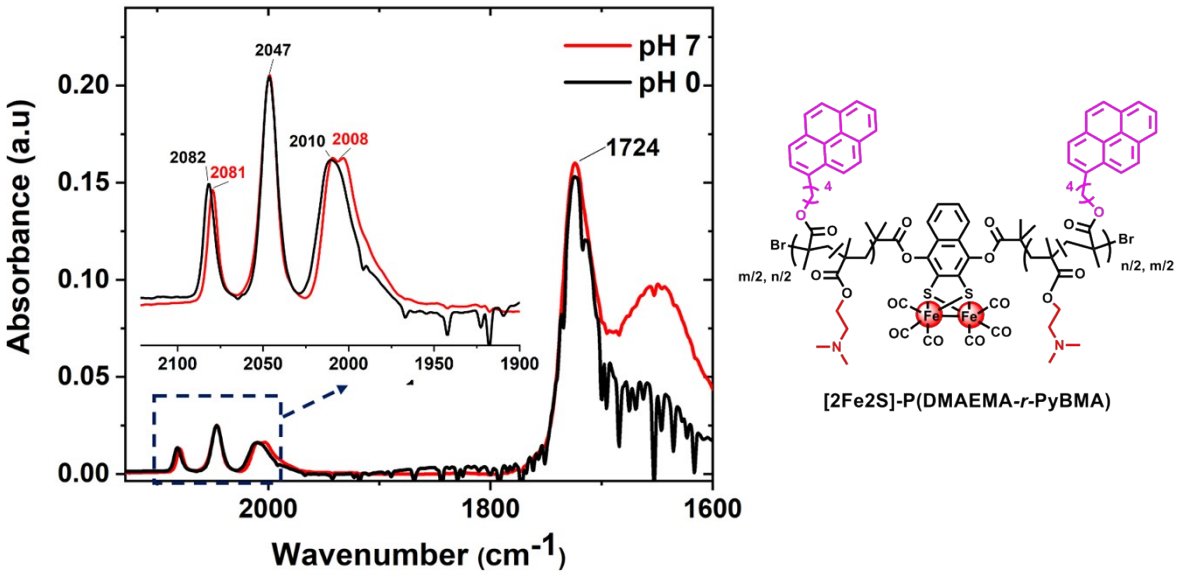

Figure S14: Infrared spectra (ATR mode) of metallopolymer [2Fe2S]-P(DMAEMA-*r*-PyBMA) at pH 0 (black trace) and pH 7 (red trace) with concentration of 100 mg mL^{-1}. For the preparation of the buffer of pH 7, 0.2 M sodium phosphate buffer was used. For pH 0, 0.5 M H_2SO4 was used.

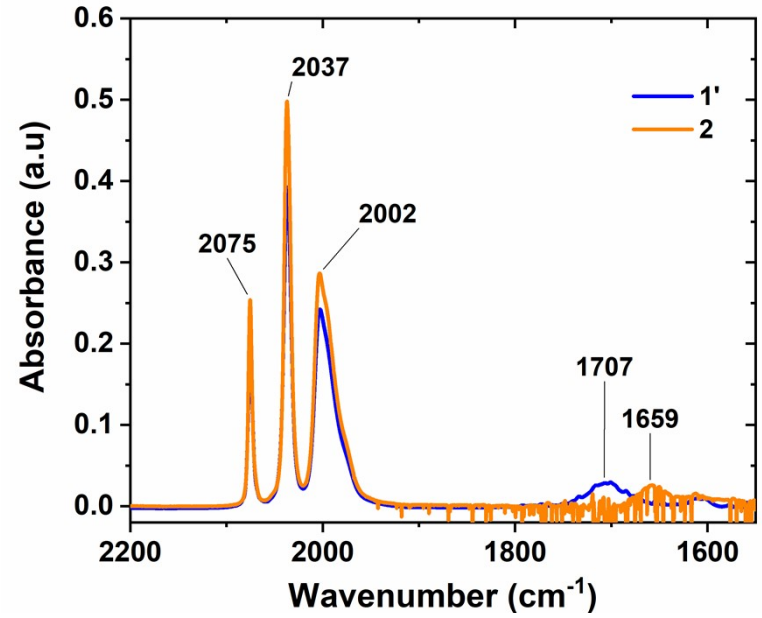

Figure S15: Infrared spectroscopy (transmission mode) of complex **1'** (blue) and **2** (orange) in $CHCl_3$ using transmission mode.

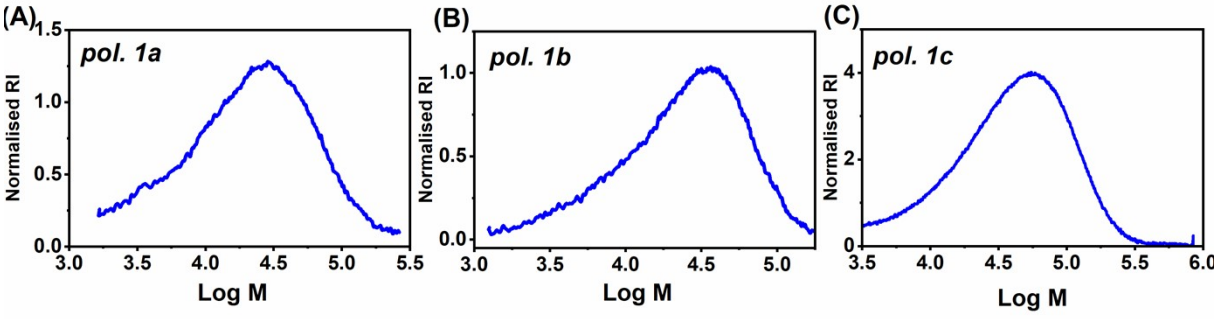

Figure S16: Size exclusion chromatogram (SEC) for metallopolymer **1a–c** in DMF.

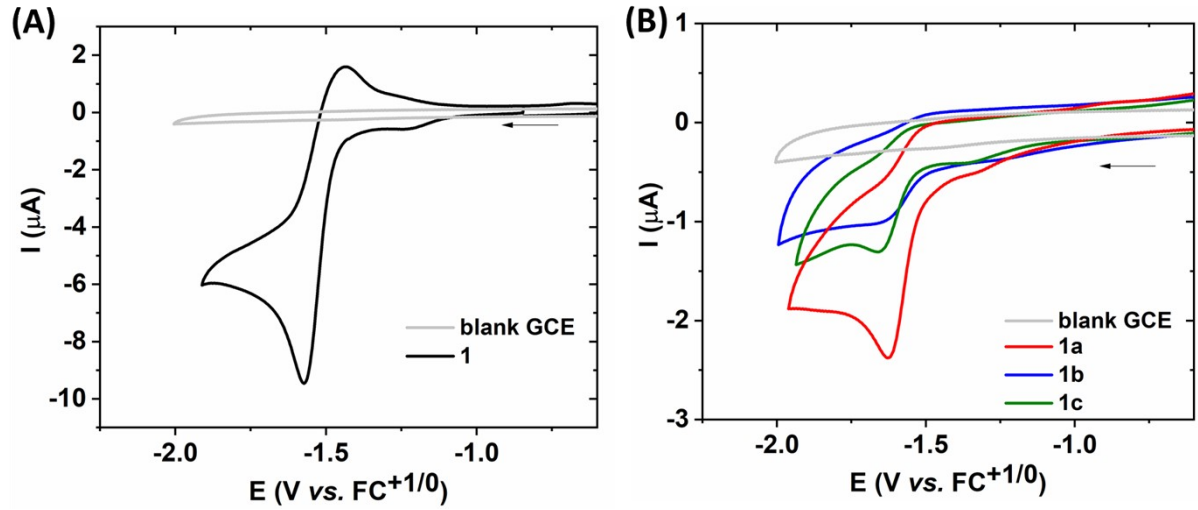

Figure S17: Cyclic voltammogram (CV) of (A) 1 mM solution complex **1** and (B) 0.5 mM solution of metallopolymers **1a–c** at 0.1 M solution of $TBAPF_6$ in CH_3CN ($\nu = 100$ mV s^{-1}). The blank glassy carbon electrode (GCE), **1**, **1a**, **1b** and **1c** are represented by grey, black, red, blue and green colours, respectively.

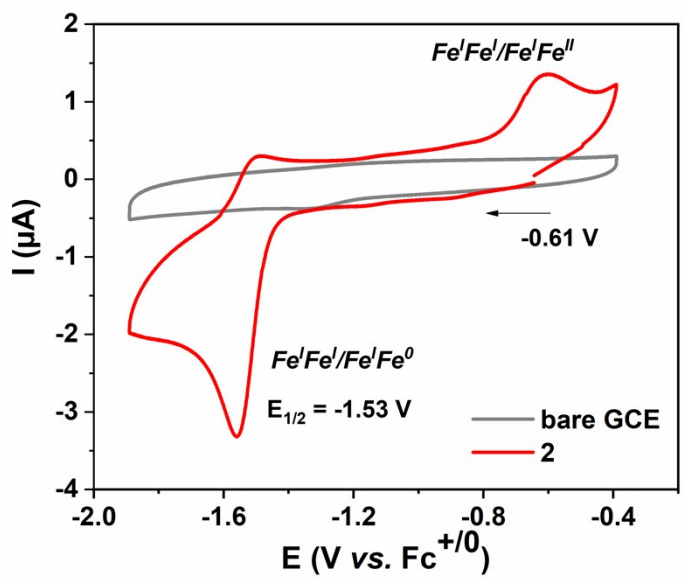

Figure S18: CV of (A) 1 mM solution complex **2** at 0.1 M solution of $TBAPF_6$ in DMF (ν = 100 mV s^{-1}). The bare glassy carbon electrode (GCE), and **2** are represented by grey and red colours, respectively. Due to limited solubility in CH3CN, the CV analysis was performed in DMF.

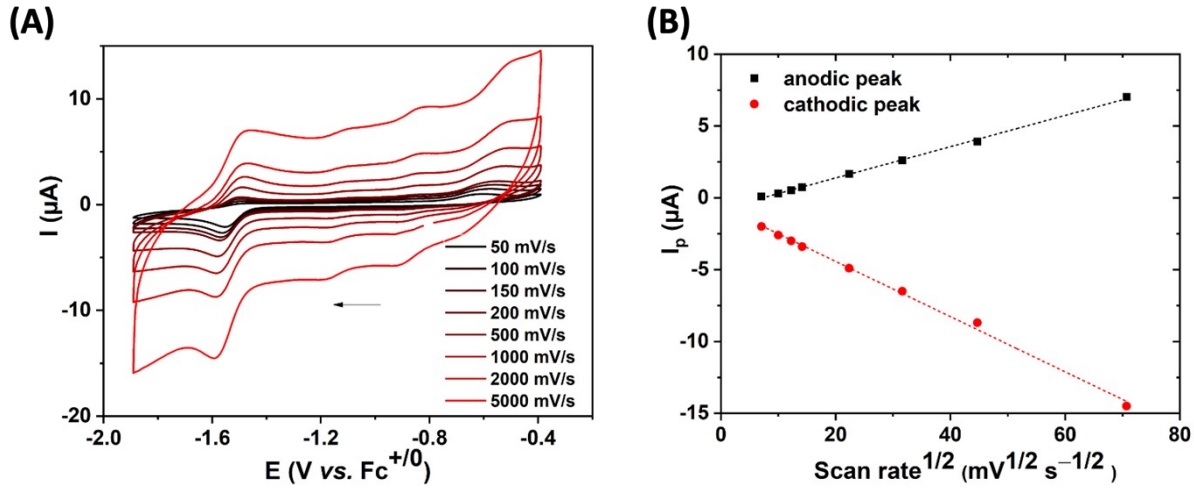

Figure S19: Scan rate dependence CV studies of 1 mM solution complex **2** at 0.1 M solution of $TBAPF_6$ in DMF (ν = 100 mV s^{-1}). (A) at scan rate between 50–5000 mV s^{-1} and (B) evolution of the redox peak current (i_p) against scan rate$^{1/2}$ ($ν^{1/2}$).

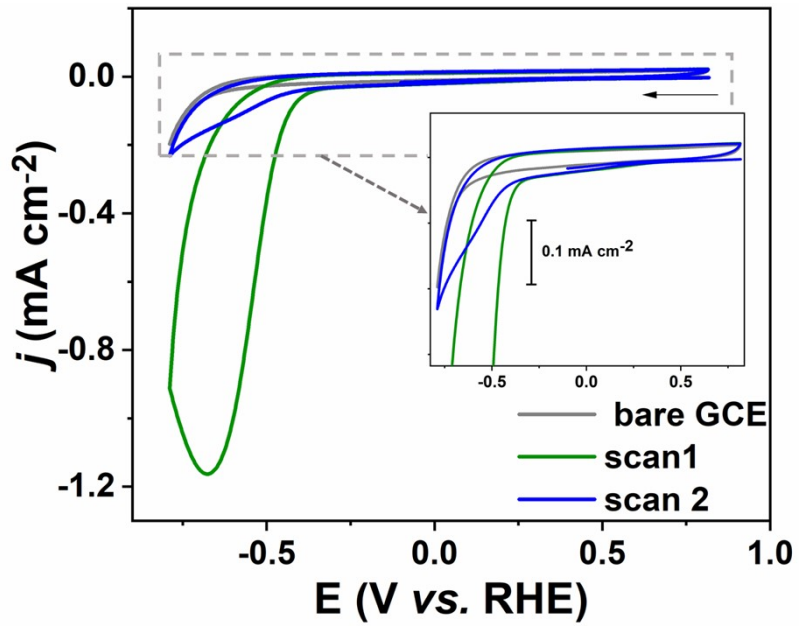

Figure S20: Rinse test assay for **1c**. Here traces represented with bare GCE (grey trace) = CV of bare glassy carbon electrode in buffer without **1c**, scan 1 (green trace) = CV on bare glassy carbon electrode in presence of 20 µM of **1c** dissolved in buffer and scan 2 (blue trace) = CV of the glassy carbon electrode after scan 1 (without polishing and gently rinsing with water), in buffer without presence of **1c**. The buffer used was 0.2 M sodium phosphate buffer, pH 7. Scan rate = 100 mV s^{-1}. It was found that about 10% of the current density was retained when comparing the catalytic currents before and after the rinse test for the metallopolymer containing the highest percentage of pyrene (~6.6%) *i.e.,* **1c**. This observation supports the notion that the observed currents are primarily related to homogenous processes under the employed conditions.

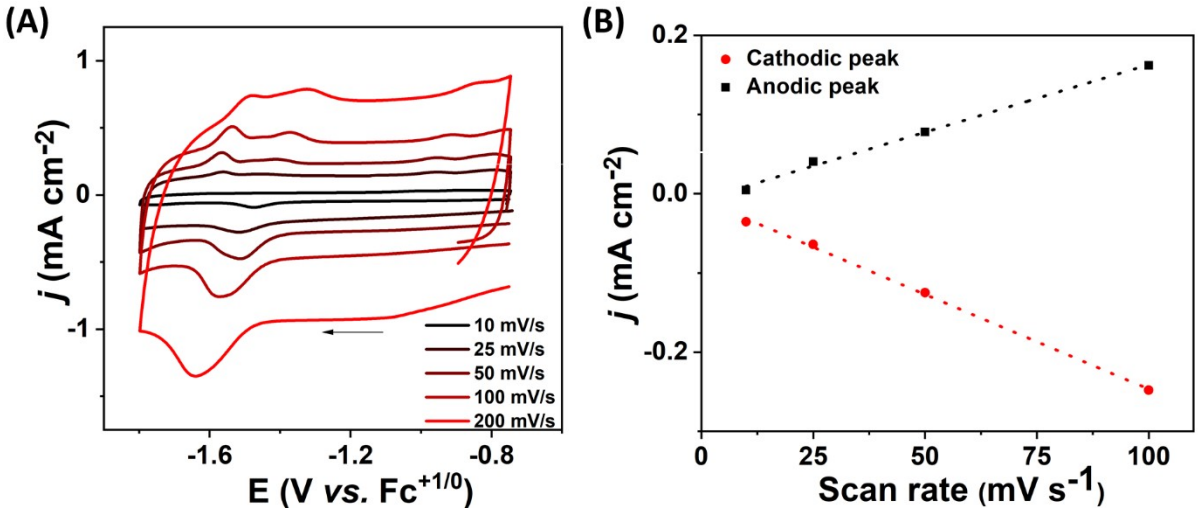

Figure S21: Scan rate dependence CV studies of **1a**/MWNT in CH_3CN at room temperature, [$TBAPF_6$] = 0.1 M. (A) at scan rate between 10–200 mV s^{-1} and (B) evolution of the redox peak current density (*j*) vs. scan rate (ν).

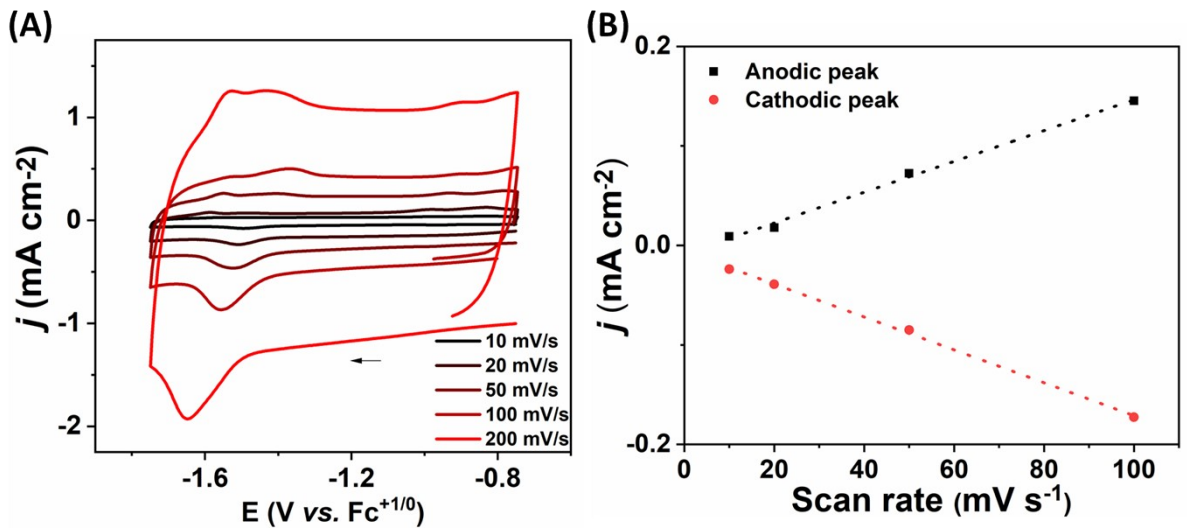

Figure S22: Scan rate dependence CV studies of **1b**/MWNT in CH_3CN at room temperature, [$TBAPF_6$] = 0.1 M. (A) at scan rate between 10–200 mV s^{-1} and (B) evolution of the redox peak current density (*j*) vs. scan rate (ν).

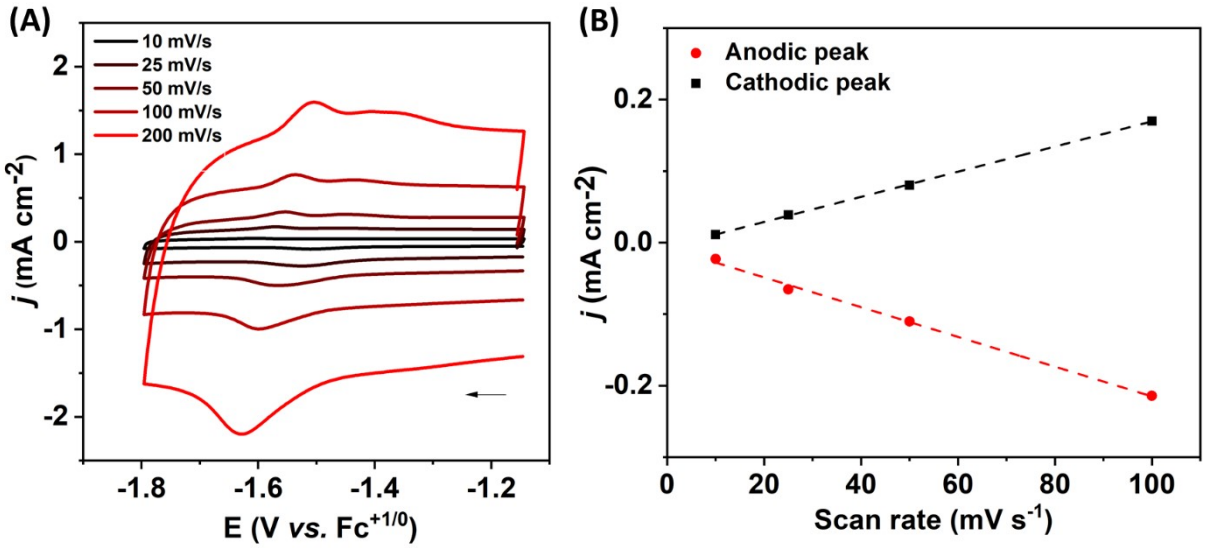

Figure S23: Scan rate dependence CV studies of **1c**/MWNT in CH_3CN at room temperature, [$TBAPF_6$] = 0.1 M. (A) at scan rate between 10–200 mV s^{-1} and (B) evolution of the redox peak current density (*j*) vs. scan rate (ν).

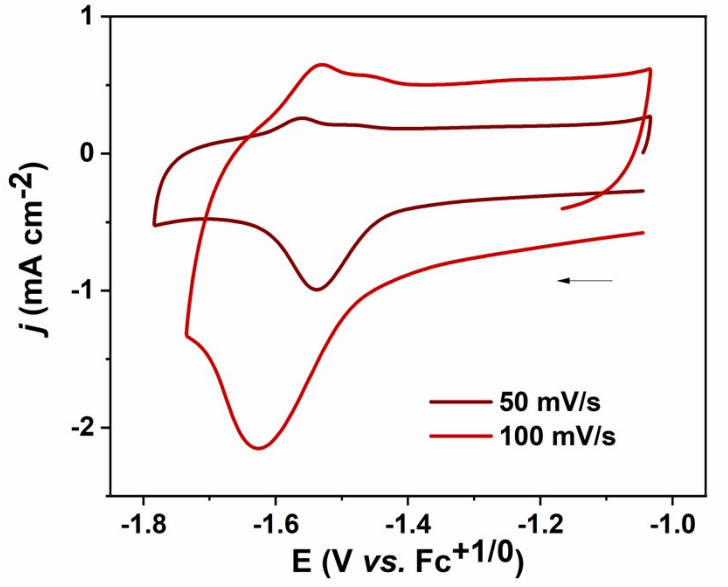

Figure S24 : CV of **2**/MWNT at 0.1 M solution of $TBAPF_6$ in CH_3CN (ν = 50 and 100 mV s^{-1}). CV at lower scan rate could not be accomplished in our hand as the catalyst was leaching very fast in electrolyte during CV.

Table S3: Analysis of heterogeneous CV of the catalysts immobilised on MWNT under organic media as shown from Figure S19-S22. $E_{1/2}$ = half wave potential, ΔE_p = peak separation or $E_{p,c} - E_{p,a}$, I_a = anodic peak current at $E_{p,a}$ = and I_c = cathodic peak current at $E_{p,c}$.

Electrodes	**$E_{½}$** **(V *vs.* $Fc^{+/0}$)**	**ΔE_p** **(mV)**	**I_a/I_c**
1a/MWNT	-1.55	40	0.98
1b/MWNT	-1.53	50	0.44
1c/MWNT	-1.57	60	0.70
2/MWNT	-1.63	35	0.54

Table S4: **Loading of the metallopolymers 1a-c and complex 2 on MWNT electrodes, as per ICP-OES measurements.** The residual standard deviation (RSD) of the measurements lied in the range between 0.2 to 2.4%.

Catalysts	**loading of active sites** **(nmol cm^{-2})**
1a	6.80 ± 0.03
1b	5.4 ± 0.1
1c	3.8 ± 0.1
2	33.6 ± 0.55

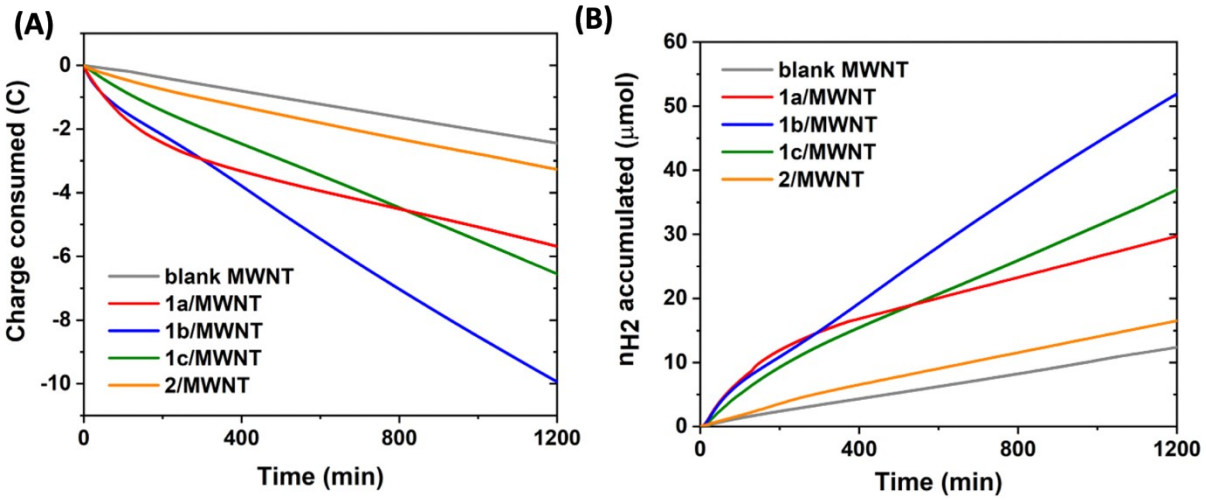

Figure S25: CA of metallopolymers **1a–c** and complex **2** immobilised on MWNT. (A) Charge consumed; (B) amount of H_2 produced during CA. The experiments were recorded by posing a potential of –0.49 V vs. RHE at working electrode in 0.2 M sodium phosphate buffer, pH 7 under continuous flow of N_2 (5 mL min^{-1}). Here, blank, **1a**, **1b**, **1c** and **2** were represented by grey, red, blue, green and orange colours respectively.

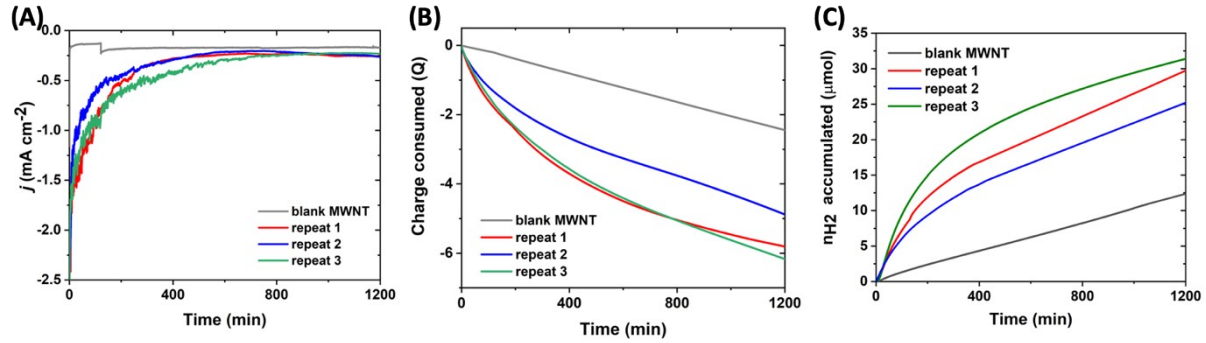

Figure S26: Repeat of the electrolysis of **1a** /MWNT. (A) current density (*j) vs.* time ; (B) charge consumed *vs*. time; (C) mol of H_2 (n_{H2}) accumulated *vs.* time during CA. The experiments were recorded by posing a potential of –0.49 V *vs.* RHE at working electrode in 0.2 M sodium phosphate buffer, pH 7 under continuous flow of N_2 (5 mL min^{-1}). Here, blank, **repeat 1**, **repeat 2** and **repeat 3** were represented by grey, red, blue and green colours respectively.

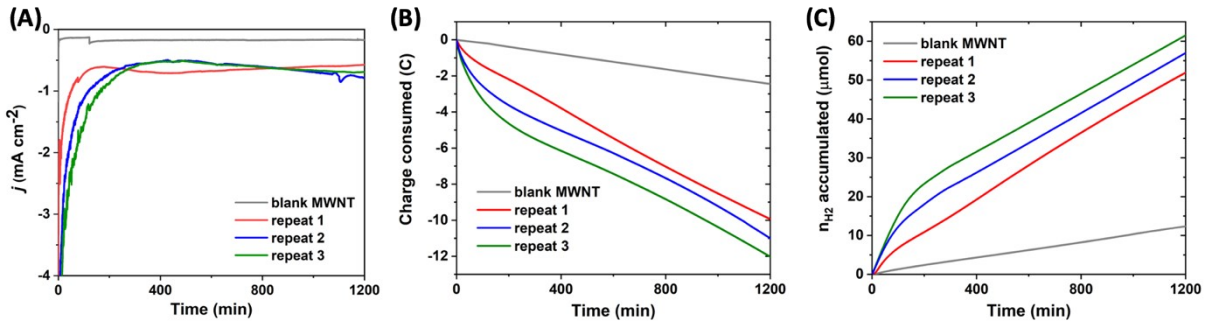

Figure S27: Repeat of the electrolysis of **1b**/MWNT. (A) current density (*j) vs.* time ; (B) charge consumed *vs*. time; (C) mol of H_2 (n_{H2}) accumulated *vs.* time during CA. The experiments were recorded by posing a potential of –0.49 V *vs.* RHE at working electrode in 0.2 M sodium phosphate buffer, pH 7 under continuous flow of N_2 (5 mL min^{-1}). Here, blank, **repeat 1**, **repeat 2** and **repeat 3** were represented by grey, red, blue and green colours respectively.

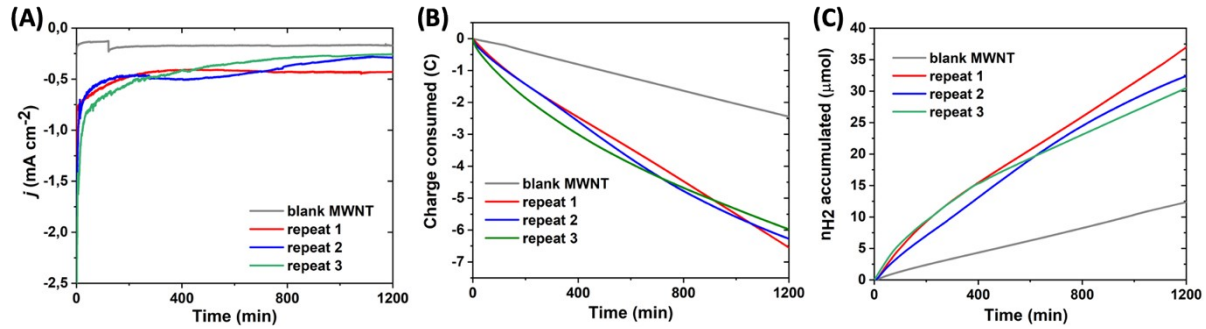

Figure S28: Repeat of the electrolysis of **1c** /MWNT. (A) current density (*j) vs.* time ; (B) charge consumed *vs*. time; (C) mol of H_2 (n_{H2}) accumulated *vs.* time during CA. The experiments were recorded by posing a potential of –0.49 V *vs.* RHE at working electrode in 0.2 M sodium phosphate buffer, pH 7 under continuous flow of N_2 (5 mL min^{-1}). Here, blank, **repeat 1**, **repeat 2** and **repeat 3** were represented by grey, red , blue and green colours respectively.

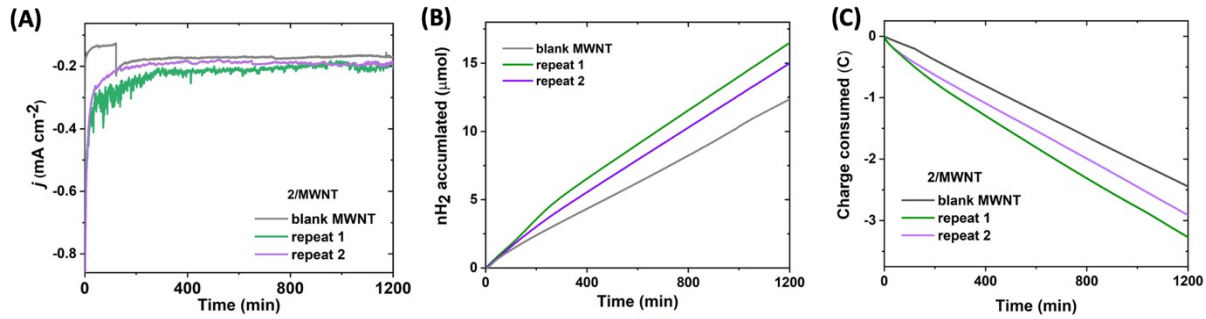

Figure S29: Repeat of the electrolysis of **2** /MWNT. (A) current density (*j*) *vs.* time ; (B) mol of H_2 (n_{H2}) accumulated *vs.* time; (C) charge consumed *vs.* time during CA. The experiments were recorded by posing a potential of –0.49 V *vs.* RHE at working electrode in 0.2 M sodium phosphate buffer, pH 7 under continuous flow of N_2 (5 mL min^{-1}). Here, blank, **repeat 1** and **repeat 2** were represented by grey, green and purple colours respectively.

Table S5: Quantitative analysis of bulk electrolysis analysis of the synthesized catalysts immobilized on MWNT shown in Figure 3 and S25. For details of calculation, see section 2.10. Here bare = bare MWNT. The standard deviation were estimated from two of the closest replicates of CA experiments for each catalyst. The replicates are shown in Figure S26– Figure S29.

Catalyst/ MWNT	***j* at t =1 min** (mA cm^{-2})	***j* at t =20 hours** (mA cm^{-2})	**n_{H2} accumulated** (µmol)	**Charge consumed** (C)	**% FE**	**% retention of *j***
bare	–0.185	–0.17	12.3	2.45	97	
1a	–2.7 ± 0.2	–0.3 ± 0.10	30 ± 1	5.8 ± 0.1	99.7 ± 0.1	8 ± 1
1b	–2.8 ± 0.1	–0.65 ± 0.10	54 ± 1	10.3 ± 0.8	99.9 ± 0.1	24 ± 2
1c	–0.9 ± 0.1	–0.35 ±0.08	35 ± 2	6.4 ± 0.1	99.1 ± 0.8	38 ± 13
2	–0.9 ± 0.1	–0.20 ± 0.01	16 ± 1	3.1 ± 0.2	98.6 ± 0.9	22 ± 4

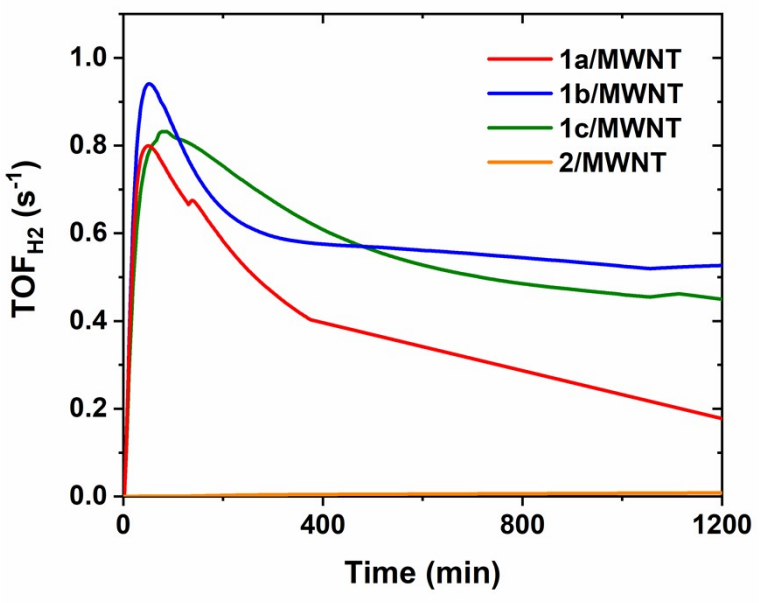

Figure S30: TOF_{H2} obtained during CA of **1a**, **1b**, **1c** and **2** while immobilised on MWNT. The experiments were recorded by posing a potential of –0.49 V *vs.* RHE at working electrode in 0.2 M sodium phosphate buffer, pH 7 under continuous flow of N_2 (5 mL min^{-1}). Here, **1a**, **1b**, **1c** and **2** were represented by red, blue, green and orange colours respectively.

Table S6: TON_{H2} and TOF_{H2} during CA by metallopolymers. We took subtracted value of n_{H2} to calculate the TON_{H2} and TOF_{H2} as a conservative value. In other words, we showed minimum value of TON_{H2} here. The standard deviation was estimated from replicates of CA experiments for each catalyst.

Metallopolymers	**Loading[a] (nmol cm^{-2})**	**TON_{H2} (× 10^4)**	**TOF_{H2} (s^{-1})**		
		20 hours	*1 hours*	*6 hours*	*20 hours*
1a	6.8	1.3 ± 0.1	0.8 ± 0.4	0.4 ± 0.1	0.18 ± 0.02
1b	5.4	3.8 ± 0.3	0.95 ± 0.20	0.6 ± 0.1	0.53 ± 0.04
1c	3.8	3.0 ± 0.4	0.8 ± 0.2	0.63 ± 0.15	0.42 ± 0.04
2	33.6	0.06 ± 0.01	0.0006 ± 0.0001	0.004 ± 0.001	0.008± 0.001

[a]calculated from ICP-OES measurements.

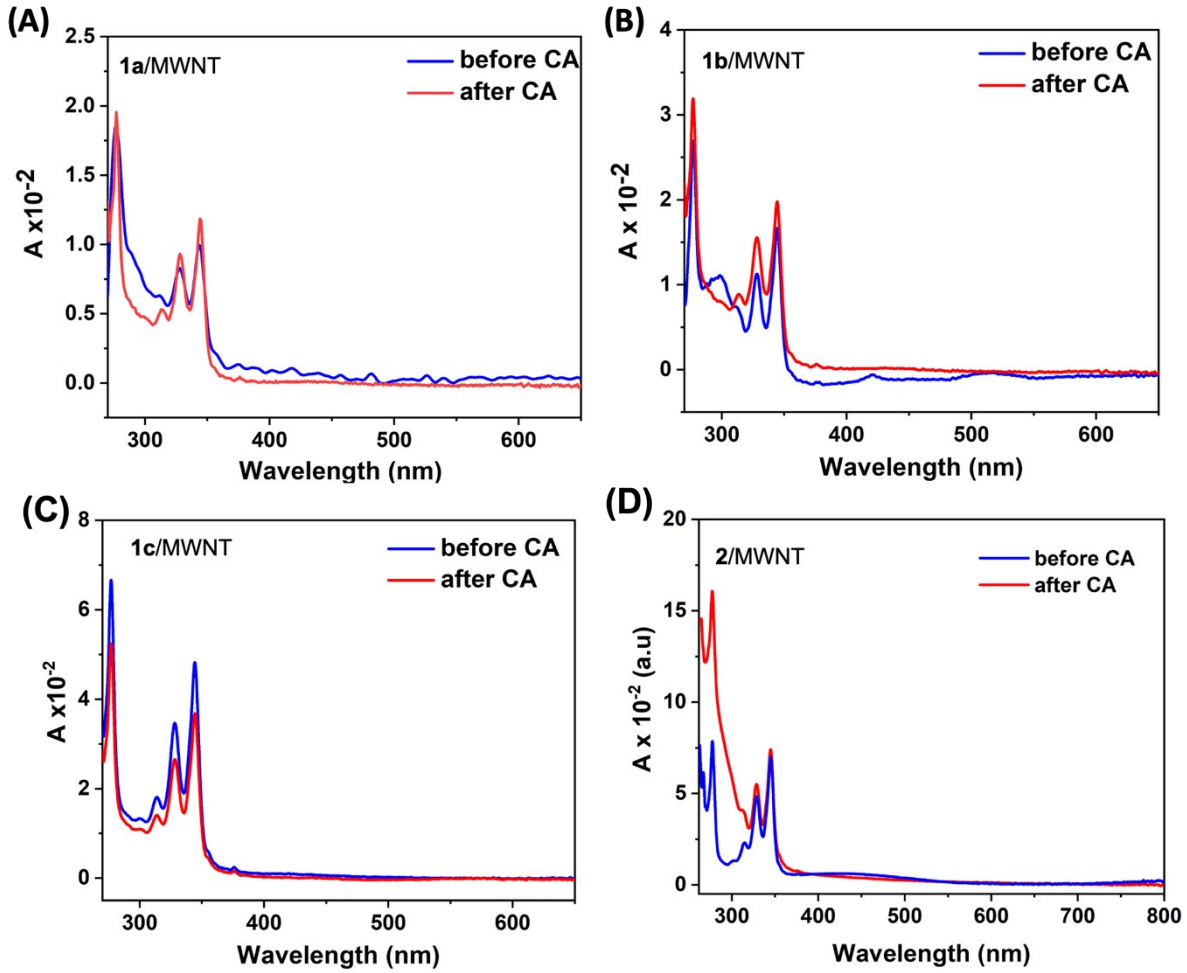

Figure S31: *Post-operando* assessment of metallopolymers using UV-vis spectroscopy. (A) **1a**/MWNT and; (B) **1b**/MWNT; (C) **1c**/MWNT; and (D) **2**/MWNT, before (blue trace), and after 20 hours (red trace) of CA. The UV-vis spectra were recorded by desorption of metallopolymers from MWNT film in 3 mL DMF. CA was performed with potential poised at −0.49 V *vs.* RHE, in 0.2 M sodium phosphate buffer of pH 7.

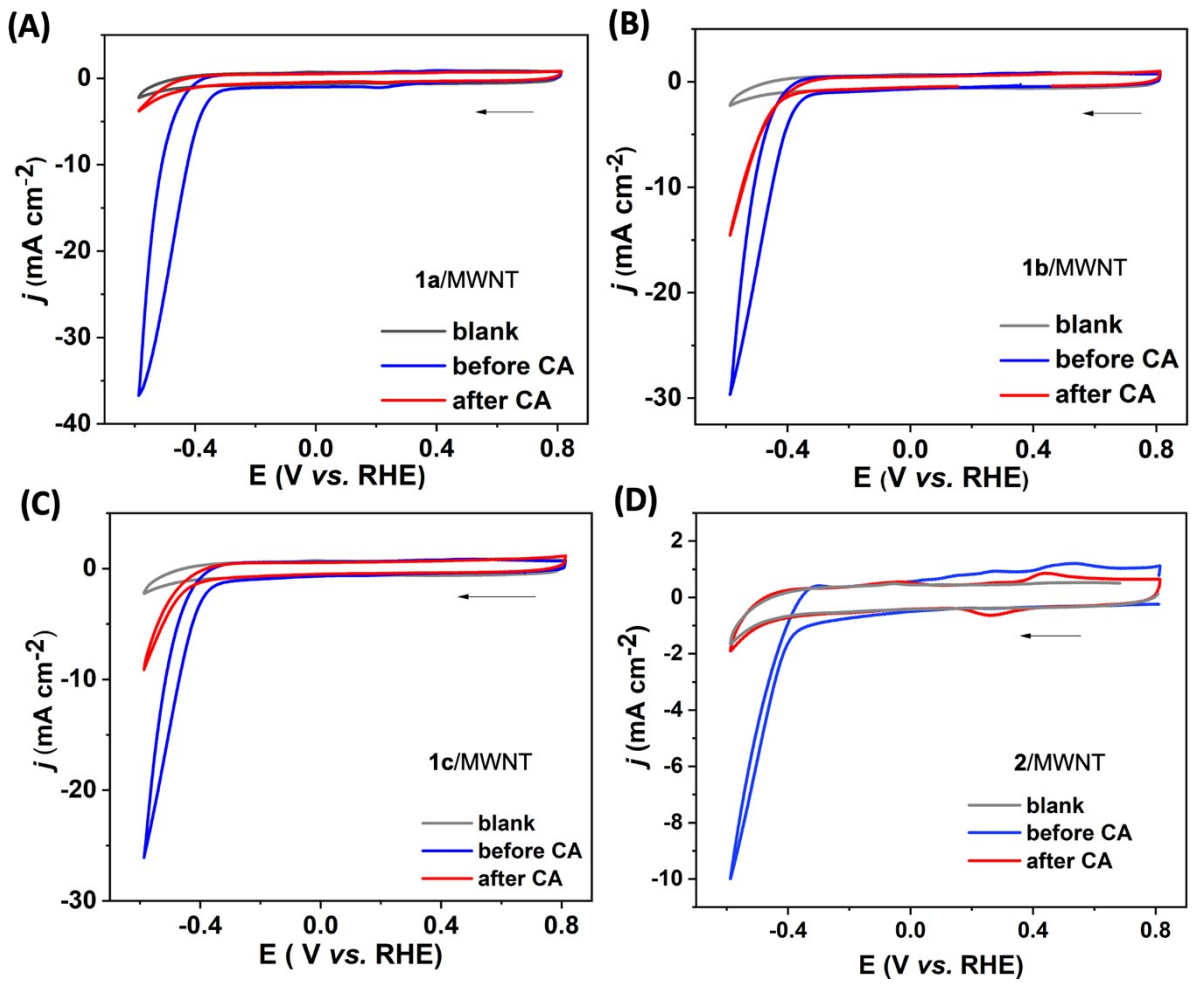

Figure S32: *Post-operando* assessment of metallopolymers and complex **2** using CV. (A) **1a**/MWNT and; (B) **1b**/MWNT; (C) **1c**/MWNT; and (D) **2**/MWNT, before (blue trace) and after 20 hours (red trace) of CA. The CV traces were recorded at ν = 100 mV s^{-1} in 0.2 M sodium phosphate buffer of pH 7. CA was performed with the potential poised at −0.49 V *vs.* RHE, in 0.2 M sodium phosphate buffer of pH 7.

Table S7: ICP-OES measurements to quantify the Fe at different stage of the chronoamperometry of **1b**/MWNT. The residual standard deviation (RSD) of the measurements lied in the range between 0.2 to 2.4%. CA was performed with potential poised at −0.49 V vs. RHE, in 0.2 M sodium phosphate buffer of pH 7.

State of the film	Loading of Fe ($\mu g\ cm^{-2}$)	loading of active sites ($nmol\ cm^{-2}$)
Before CA	0.61 ± 0.03	5.40 ± 0.3
After 1 hour of CA	0.54 ± 0.03	4.8 ± 0.3
After 3 hours of CA	0.37 ± 0.05	2.3 ± 0.4
After 20 hours of CA	0.18 ± 0.03	1.6 ± 0.3

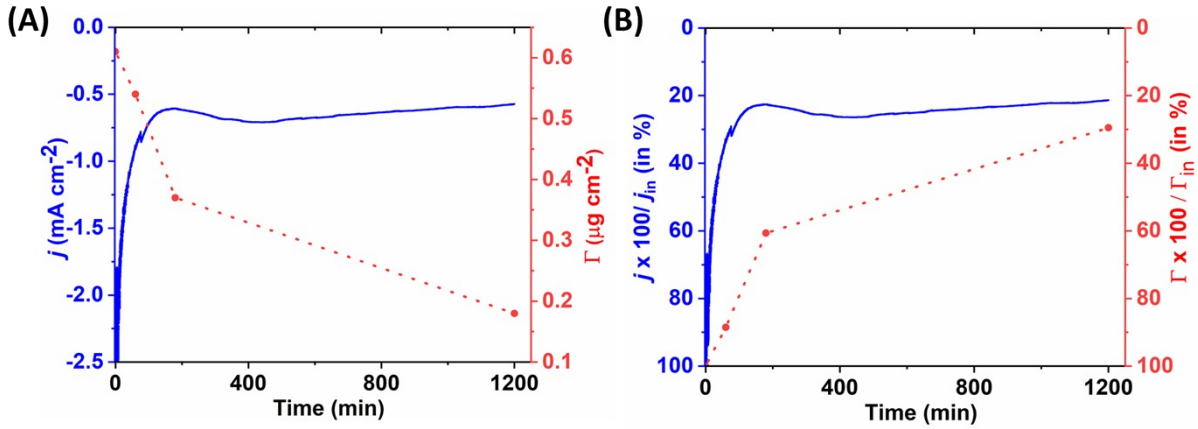

Figure S33: (A) CA of **1b**/MWNT (blue trace) and loading of Fe on MWNT (red trace) over time during CA; and (B) corresponding percentage (%) of current density and % of loading over time during CA. CA was performed with potential poised at −0.49 V *vs.* RHE, in 0.2 M sodium phosphate buffer of pH 7. Here, Γ = the active site loading and Γ_{in} = active site loading at the beginning of CA, j_{in} = current density at the beginning of CA.

4. References

(1) Zamader, A.; Reuillard, B.; Marcasuzaa, P.; Bousquet, A.; Billon, L.; Espí Gallart, J. J.; Berggren, G.; Artero, V. Electrode Integration of Synthetic Hydrogenase as Bioinspired and Noble Metal-Free Cathodes for Hydrogen Evolution. *ACS Catal.* **2023**, *13*, 1246–1256. https://doi.org/10.1021/acscatal.2c05175.

(2) Heine, D.; Pietsch, C.; Schubert, U. S.; Weigand, W. Controlled Radical Polymerization of Styrene-Based Models of the Active Site of the [FeFe]-Hydrogenase. *J. Polym. Sci. A Polym. Chem.* **2013**, *51* (10), 2171–2180. https://doi.org/10.1002/pola.26584.

(3) Gao, W.; Song, L.-C.; Yin, B.-S.; Zan, H.-N.; Wang, D.-F.; Song, H.-B. Synthesis and Characterization of Single, Double, and Triple Butterfly [2Fe2E] (E = Se, S) Cluster Complexes Related to the Active Site of [FeFe]-Hydrogenases. *Organometallics* **2011**, *30* (15), 4097–4107. https://doi.org/10.1021/om200395g.